ChemComm

Bipolar electrochemistry in synergy with electrophoresis: Electric field-driven electrosynthesis of anisotropic polymeric materials

Journal:	*ChemComm*
Manuscript ID	CC-FEA-09-2020-006204.R1
Article Type:	Feature Article

ARTICLE

Bipolar electrochemistry in synergy with electrophoresis: Electric field-driven electrosynthesis of anisotropic polymeric materials

Received 00th January 20xx,
Accepted 00th January 20xx

DOI: 10.1039/x0xx00000x

Naoki Shida,[a] Shinsuke Inagi[a,b]*

Bipolar electrochemistry, which refers to an electrochemical system at a wireless electrode driven under an applied electric field, has been recognized as not only a simple subset of conventional electrosynthetic systems but a reaction system with a highly unique nature. One notable feature is the presence of the electrophoretic effect due to the low electrolyte concentration. The electrophoresis enhances the mass transfer of ionic species in a specific direction, thus enabling the efficient construction of anisotropic materials. In this Feature Article, we summarized our recent reports on the fabrication of anisotropic conductive polymer fibers and films via bipolar electrochemistry in synergy with the electrophoretic effect.

1. Introduction

The last two decades have witnessed a flourishment of bipolar electrochemistry.[1–3] Bipolar electrochemistry is an electrochemical system with a wireless electrode (bipolar electrode, BPE) driven under an applied electric field. BPEs are known for various unique features, such as their wireless nature, symmetry breaking, anisotropy, and potential gradient, most of which are not observed in conventional two- or three-electrode systems. The technology of bipolar electrochemistry has a long history, including an industrial application for the electrosynthetic process commercialized by BASF.[4] Recent examples of the application of bipolar electrochemistry span a wide range of fields, including materials synthesis, organic synthesis, sensors, combinatorial chemistry, locomotion of microscale objects, polymer actuators, microfluidics, electrochemiluminescence, and bioimaging. These examples, along with explanations of the fundamental theory of bipolar electrochemistry, have been summarized in reviews by various groups.[1–3,5–9]

In the present article, we describe our recent work on the fabrication of anisotropic materials via bipolar electrochemistry, with special emphasis on the synergetic effect of electrophoresis. In electrophoresis, ions migrate in a specific direction under an electric field. Because an intense electric field plays a critical role in both bipolar electrochemistry and electrophoresis, these two concepts are clearly connected. We showcase our design of bipolar electrochemical systems based on this concept and discuss the benefits of electrophoresis, especially in materials synthesis. Our aim in the present article is to shed light on the importance of the inherently highly compatible but relatively overlooked phenomena of electrophoresis and bipolar electrochemistry.

We refer readers to the review of Kuhn and coworkers on capillary-assisted bipolar electrochemistry, which provides a summary of bipolar electrochemistry in microcapillaries with electroosmotic flow.[10] The present review focuses more on the electrophoretic phenomenon in a bulk solution; thus, this Feature Article addresses complementary aspects of microfluidic systems.

2. Principles

In this section, we highlight the features of bipolar electrochemistry through comparison with conventional electrolytic systems and then discuss the basic theoretical aspects of bipolar electrochemistry.

Conventional electrolytic systems are designed to induce electron transfer between driving electrodes and in-solution substrates. Conventional electrolysis generally employs a high concentration of supporting electrolyte (>0.1 M) to effectively form electrical double layers upon the application of an electrical bias. The thickness of the electrical double layer is on the order of several nanometers, in which a steep gradient of the solution potential is formed to ensure electron transfer between the electrode and the substrate (Figure 1a). By contrast, the electrical double layers are not fully formed in a solution with a low concentration of supporting electrolyte; thus, an electric field is instead formed across the bulk solution. In this situation, electron transfer barely occurs at the surfaces of the driving electrodes; however, a conductor placed between the electrodes can act as a BPE that simultaneously participates in oxidation and reduction at its terminals (Fig. 1a).

The electric field can be experimentally measured using a two-terminal voltmeter as the slope of the IR-drop (Fig. 1b). The sum of the interface potential differences at both edges of a conductor (ΔV_{BPE}) is proportional to the length of the BPE and the strength of the electric field (Fig. 1b). The redox reactions proceed on a

[a] Department of Chemical Science and Engineering, School of Materials and Chemical Technology, Tokyo Institute of Technology, 4259 Nagatsuta-cho, Midori-ku, Yokohama 226-8502, Japan.
[b] PRESTO, Japan Science and Technology Agency (JST), 4-1-8 Honcho, Kawaguchi, Saitama 332-0012, Japan.

BPE when ΔV_{BPE} is greater than the potential difference between the target redox reactions; thus ΔV_{BPE} is a useful index to estimate the extent of the bipolar electrochemical reactions.

The electric field is also proportional to the mobility of the ionic species involved in the electrophoresis (Fig. 1c). The direction of electrophoretic migration is forward with respect to the electric field in the case of the cationic species, whereas anionic species migrate in the opposite direction. Hence, cationic species approach cathodic and anodic poles of a BPE from the side of the driving anode, whereas anionic species approach from the side of the driving cathode. Thus, the configuration of BPEs must be carefully considered in bipolar electrolysis with ionic reactants.

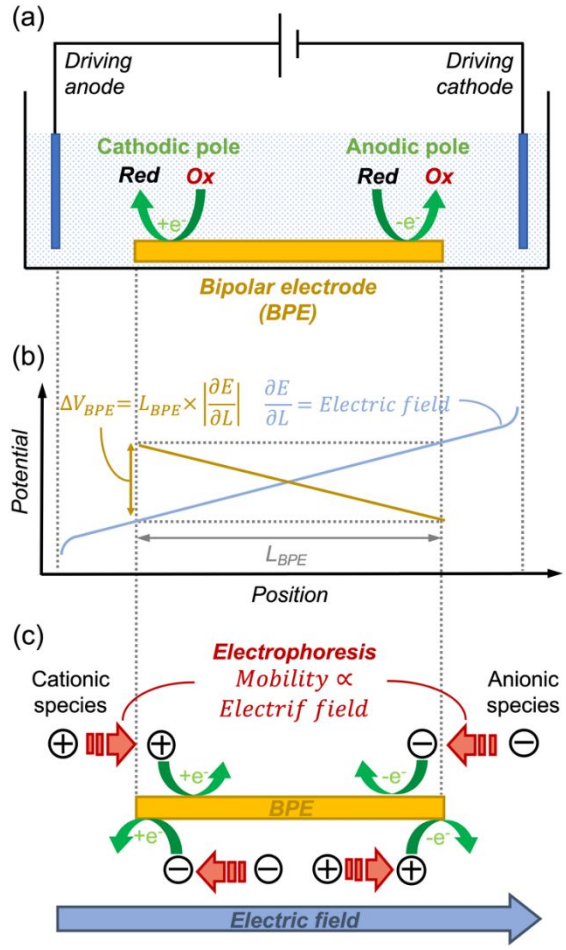

Fig. 1 General concept and theoretical background of bipolar electrochemistry and electrophoresis in bipolar electrolysis: (a) setup of the electrochemical cell with a BPE; (b) conceptual diagram of the electric field and potential on the BPE; and (c) concept of bipolar electrochemistry in synergy with electrophoresis.

3. Setup for Bipolar Electrochemistry

We here briefly summarize the variables related to the setup of bipolar electrolysis. First, BPEs are classified into two main systems: open and closed BPEs. The open BPE system is a simple and thus common mode of BPEs, where a conductor is placed between the driving electrodes without separating the chamber. In a closed BPE system, an insulating material divides the cell into two or more chambers connected together by conductors, *i.e.*, BPEs. In an open BPE system, ions and substrates (in solution) and electrons (in BPEs) are all mobile. By contrast, the movement of in-solution species is blocked by the separator in a closed BPE system; thus, only the electrons can migrate across the chamber. The closed BPE requires more complicated setup than the opened one, while the closed BPE enables the use of different types of solvents and reagents in two chambers without mixing.

The shape of the cell is also an important variable in bipolar electrochemistry, and various cells have been proposed for this application (Fig. 2b). In addition to a simple linear setup, a U-shaped cell and a cylindrical cell have also been reported. Both the U-shaped and cylindrical cells have an insulating wall to partially (*i.e.*, not completely) separate the electrolyte, which enables an intentional distortion of the electric field. In a linear cell, the electric field is also linear;[11] however, U-shaped and cylindrical cells form sigmoidal[12–16] and circular[17–19] electric fields, respectively. The sigmoidal electric field in a U-shaped cell enlarges the effective surface area on a BPE, where the potential is above the threshold for target redox reactions, compared to the case in a linear cell. A cylindrical cell uniquely applies electrical potential on a BPE in a site-selective manner.[17–19] Such engineering of the electric field enables gradient modification and patterning.[12–19] The electric fields can be computationally simulated using COMSOL.[18,19] Xu and co-workers have also proposed conceptually new types of BPE cells (Fig. 2b). They prepared an insulating plastic label with holes on a single electrode to construct a microelectrochemical cell, and applied electrochemical voltage by using driving electrodes attached outside the plastic label.[20] Xu also reported unique transmitter-based BPE systems, which enable driving a BPE without soaking driving electrodes in a reaction solution.[21,22]

There is almost no limitation to the shape of BPEs, as long as they are conductive. Numerous reports describe BPEs with plate, bead, and wire shapes. As formulated in Fig. 1b, ΔV_{BPE} is proportional to the length of a BPE; thus, smaller BPE materials require stronger electric fields. Also, small objects such as beads easily float and rotate in liquid electrolytes. Thus, bipolar electrochemistry can induce migration of microscale objects.[23,24] The site-selective modification of such microscale objects requires that they be fixed using a nonconvectional material such as agarose gel.

The configuration of a BPE is also an important variable (Fig. 2). In principle, all conductors work equally well under the same electric field; thus, array configurations are as widely used as common single BPE systems. BPE arrays are especially powerful for combinatorial assessments using an electrochemiluminescence (ECL) method as a wireless readout.[25,26] Split BPEs, where two distinct conductors are wired to perform as a single BPE, are also a common configuration option. The most important benefit of a split BPE is that reactions on the BPE can be monitored using ammeters.[27] In addition, a split BPE can substantially reduce the amount of conducting material required, which is a great advantage when the BPEs of interest are made of noble metals.

ARTICLE

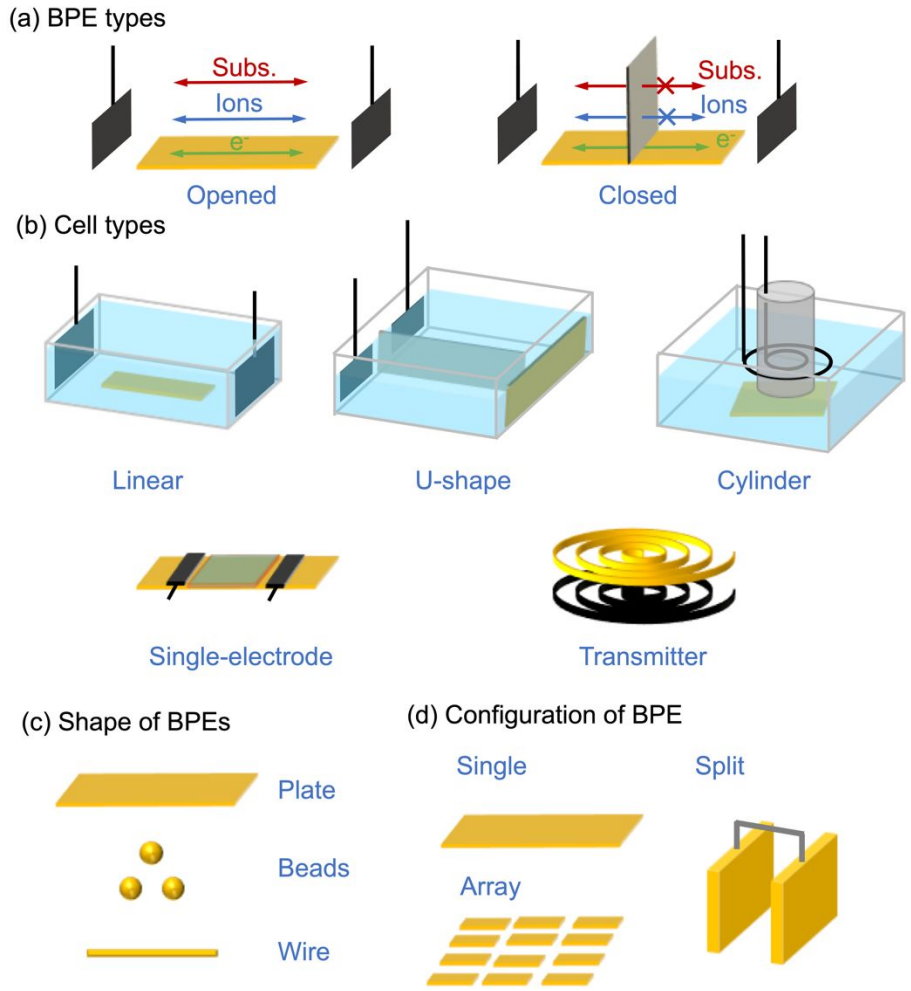

Fig. 2 Representative variables in the setup of bipolar electrochemistry: (a) open and closed BPE systems; (b) cell types; (c) shapes of BPEs; and (d) configurations of BPEs.

4. Synergetic Effect of Electrophoresis in DC-Bipolar Electrolysis

The vast majority of bipolar electrochemistry has been conducted under an applied direct current (DC). DC-bipolar electrochemistry effectively promotes the migration of ionic species in one direction. An early notable achievement was reported in the late 1990s by Bradley and coworkers, who used Cu particles as BPEs.[28–31] The Cu particles were placed nearby and subjected to the DC-bipolar condition. The anodic dissolution of metallic Cu and cathodic electroplating led to the dendritic deposition of Cu metal parallel to the direction of the external electric field, and the Cu particles were eventually electrically connected to each other. Their strategy is referred to as programmable hard-wiring.[32]

From the late 2000s to the 2010s, bipolar electrochemistry gained renewed attention, especially for the synthesis of asymmetric and anisotropic materials, as represented by the pioneering works by Kuhn and coworkers,[33–35] Björefors and coworkers,[36,37] and our group.[12–19] These examples were conducted under an applied direct current, thus inducing a gradient change of the electrical potential irrespective of time.

Kuhn and coworkers used bipolar electrochemistry to fabricate various Janus-type materials by electroplating or electrografting. These systems utilize ionic species (metal ions or aryldiazonium ion) for modification;[33–35,38] thus, the electrophoresis should proceed concomitantly. A representatively unique result was observed during the bipolar electroplating of Au or glassy carbon (GC) beads with anionic metal salts, *i.e.*, $AuCl_4^-$ or $PtCl_6^{2-}$, where a ring-shaped modification was observed rather than a

Janus-type, which is very difficult to achieve by other methods (Fig. 3).[39] The authors attributed this phenomenon to the electrophoretic migration of anionic salts, which resulted in the migration of anions from the cathodic surface of BPE beads and subsequently limited the reaction with the ions to only a certain edge. These unique diffusion and bipolar electroplating systems were successfully simulated using COMSOL.

The synergetic effect of electrophoresis under DC-bipolar conditions was also found to be efficient for templated electrolysis. Electrolysis with a hard template such as an anodized aluminum oxide (AAO) membrane is a simple and straightforward method to prepare a one-dimensional (1D) nanostructure standing perpendicularly on the electrode surface. However, the high aspect ratio and narrow space in the AAO membrane greatly limit the diffusion of chemical species, which disfavors the formation of nanorods and instead results in tubular structures. Such hollow nanotubes are mechanically fragile and thus tend to collapse upon the removal of the template. In this context, the development of a method to enhance the diffusion of chemical species in nanopores is strongly desired.[40,41] To this end, our group conducted electrophoresis-assisted bipolar electrolysis in the nanopores of an AAO membrane (Fig. 4a).

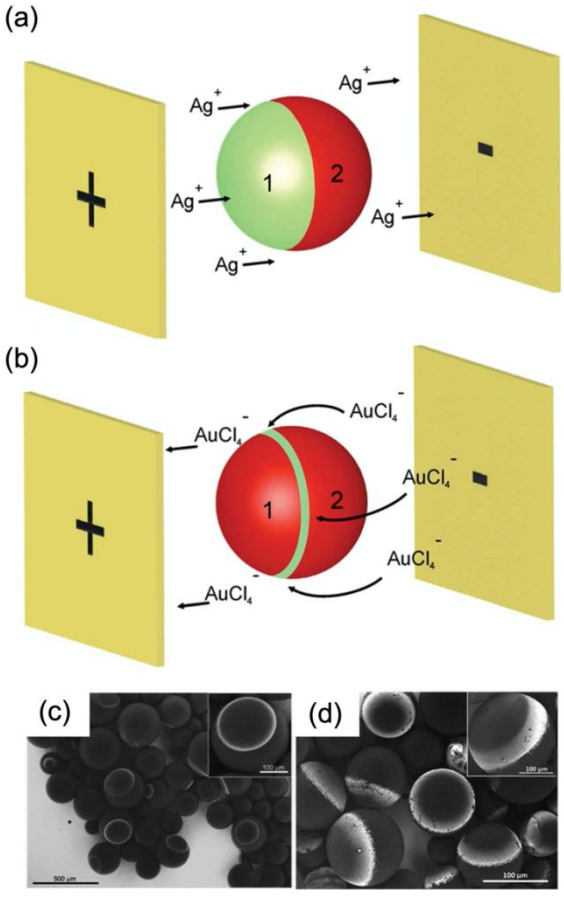

Fig. 3 Electrodeposition of metals onto bipolar bead electrodes, as reported by Kuhn and coworkers:[39] (a,b) conceptual illustration of electrodeposition using (a) Ag^+ cations or (b) $AuCl_4^-$ anions. (c, d) SEM images of GC-beads modified with (c) Pt rings or (d) Au rings. Reproduced with permission from ref. 39. Copyright 2014 Royal Society of Chemistry.

The AAO membrane-fixed BPEs were prepared according to the following procedure. One side of an AAO membrane (200 nm pore size, 60 mm thickness, 13 mm diameter) was sputtered with Au (200 nm) and then attached to an indium-doped tin oxide (ITO) substrate using epoxy glue; the substrate was connected to a pristine ITO plate to form a split BPE (Fig. 4b). We first demonstrated the electrodeposition of metal ions from precursors such as $CoCl_2 \cdot 6H_2O$ and $PtCl_2$.[42] The electrolyte solution contained metal salts and hydroquinone (HQ) in acetonitrile (MeCN). When a sufficiently large ΔV_{BPE} was applied to induce reduction of the metal ions and oxidation of HQ, Co nanorods and Pt nanorods were observed by scanning electron microscopy (SEM) after the AAO template was removed (Fig. 4c). A standing structure was observed in both cases, indicating the formation of densely packed and thus mechanically strong nanorods.

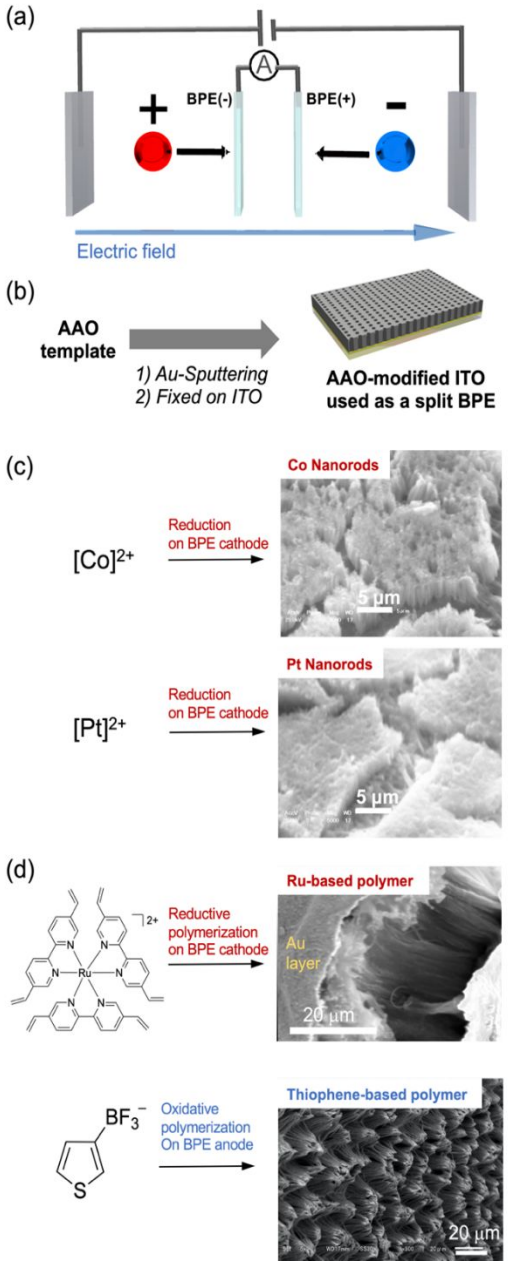

Fig. 4 Electrophoresis-assisted formation of 1D materials by DC bipolar electrolysis using AAO templates:[42,43] (a) conceptual illustration; (b) preparation of AAO-modified ITO electrode, which was used as a BPE in the split-BPE configuration; (c) reductive deposition of Co^{2+} and Pt^{2+} ions and the corresponding SEM images of the resultant nanorods thereof.[42] Reproduced with permission from ref. 42. Copyright 2018 Royal Society of Chemistry; (d) reductive or oxidative polymerization of a Ru-containing vinyl monomer or thiophene monomer.[43] Reproduced with permission from ref. 43. Copyright 2020 American Chemical Society.

On the basis of this concept, we also demonstrated the formation of nanofibers via templated bipolar electrolysis.[43] In this case, an ionic monomer such as $[Ru(dvbpy)_3](PF_6)_2$ (dvbpy = 5,5′-divinyl-2,2′-bipyridine) or potassium 3-thiophenetrifluoroborate was used. $[Ru(dvbpy)_3](PF_6)_2$ is known to polymerize upon reduction, whereas 3-thiophenetrifluoroborate can be polymerized anodically. As expected, polymer nanowires standing perpendicularly against the substrate were observed by SEM.

In both cases of metal nanorod and polymer wire formation, control experiments under constant-potential electrolysis, *i.e.*, conventional templated electrolysis, resulted in a collapsed structure upon removal of the AAO template, presumably because of the mechanical fragility of the tubular structure. As described in the preceding section, a high concentration of electrolyte (0.1 M) was used in the conventional electrolysis; thus, the generated electric field should be limited because of the slight effect of electrophoresis. Consequently, the limited diffusion of substrates into nanopores was critical for the formation of nanostructures. By contrast, the templated bipolar electrolysis yielded successful nanostructures, suggesting a substantial benefit of the synergetic effect of electrophoresis.

5. Synthesis of PEDOT Fibers by AC-bipolar Electropolymerization Assisted by Electrophoresis

In 2014, our group reported the bipolar electrochemical deposition of Au onto GC beads under an applied alternating current (AC).[44] The resultant beads showed symmetric electroplating of Au on both poles, reflecting the symmetric nature of the AC-bipolar system. Interestingly, ΔV_{BPE} measured during the electrolysis showed a highly stable profile, in contrast to the rapid decrease in ΔV_{BPE} during the time course of the electrolysis under the DC condition. One reason for the stable electric field in the AC-bipolar system could be the suppression of the overoxidations/reductions on the driving electrodes.

After reporting the aforementioned findings, we serendipitously applied this system to electropolymerization (Fig. 5).[45] Au wire (ϕ = 50 μm, length = 20 mm) was used as a BPE, which was placed between the Pt driving electrodes with an electrolyte solution containing 1 mM Bu_4NClO_4/MeCN. 3,4-Ethylenedioxythiophene (EDOT) and benzoquinone (BQ) were both added at a concentration of 50 mM and 5 mM, respectively, to the solution as a monomer and a sacrificial reagent, respectively. A 5 Hz square-wave AC was applied with ΔV_{BPE} = 8.3 V. The anodic and cathodic reactions are represented in Fig. 5a. The EDOT monomer was anodically oxidized, and the electrons were carried to the cathodic pole, where they reduced BQ to HQ. This method was applied to other EDOT derivatives such as EDOT with methyl and *n*-decyl groups to give the corresponding polymer fibers with different microstructures, as confirmed by SEM observations.[45]

The observation that the polymer fibers continuously propagated from their terminus indicates that all of the poly(3,4-ethylenedioxythiophene) (PEDOT) fibers were electrically conductive. Thus, this methodology is applicable as a novel wiring technology for conductive materials, including the wiring of integrated circuits. To this end, we have demonstrated the connection of independent Au wires with different lengths. Au wires W1–W3 were subjected to bipolar conditions. At the beginning of the electrolysis, the PEDOT fibers started to grow only at the termini of W1, whose length was sufficient to induce redox reactions. Immediately after W1 and W2 were connected by the PEDOT fibers, the fiber growth from W1 paused and new fibers started to grow from the other terminus of W2. Subsequently, W2 was electrically connected to W3 by the PEDOT fibers. This preliminary experiment demonstrated not only the potential of the current method as a new wiring technology but also a new concept to sequentially "activate" a conductive material through dynamic connection with a propagating end.

The proposed mechanism for the formation of PEDOT fibers under AC-bipolar conditions is illustrated in Fig. 6. The oxidized monomers react to give oligomers, which are more readily oxidized at the anodic pole because of the expansion of the π-system. Hence, positively charged EDOT oligomers are generated. These oligomers are still soluble in the electrolyte solution and therefore migrate back and forth parallel to the direction of the electric field via the electrophoretic effect. After further oxidative condensation, PEDOT is precipitated out, yielding PEDOT fibers. Under the principles of bipolar electrochemistry, the highest reaction rate occurs at the very edge of the electrode. Thus, the termini of the PEDOT fibers become the selective sites for polymer propagation. The electrophoresis is responsible for the directed propagation of PEDOT fibers.

AC-bipolar electropolymerization is a next-generation electropolymerization method that enables the preparation of shape-controlled conducting polymers in the absence of a template.[46]

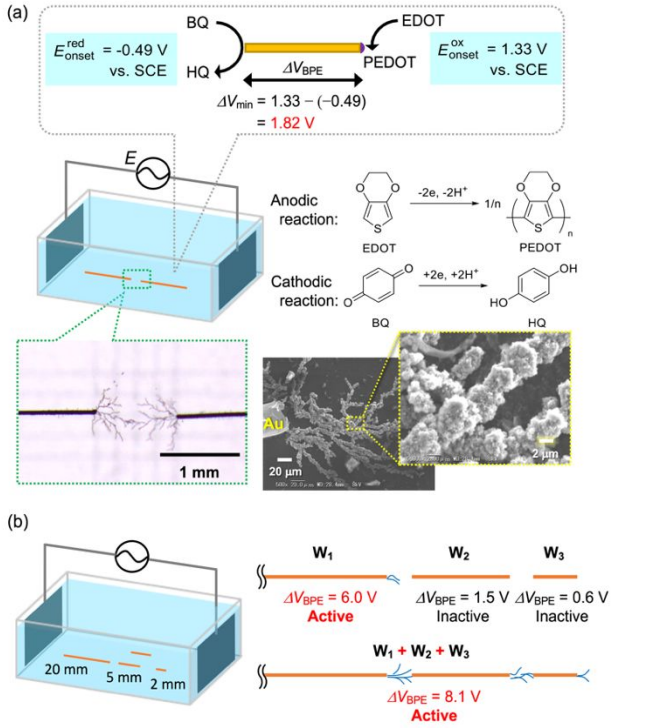

Fig. 5 Fabrication of PEDOT fibers by AC-bipolar electrolysis.[45] (a) Schematic of the AC-bipolar system for PEDOT fiber formation, and optical and SEM images of the resultant PEDOT fibers. (b) "Sequential activation" of Au wires upon connection with BPEs via PEDOT fibers. Reproduced with permission from ref. 45. Copyright 2016 Springer Nature.

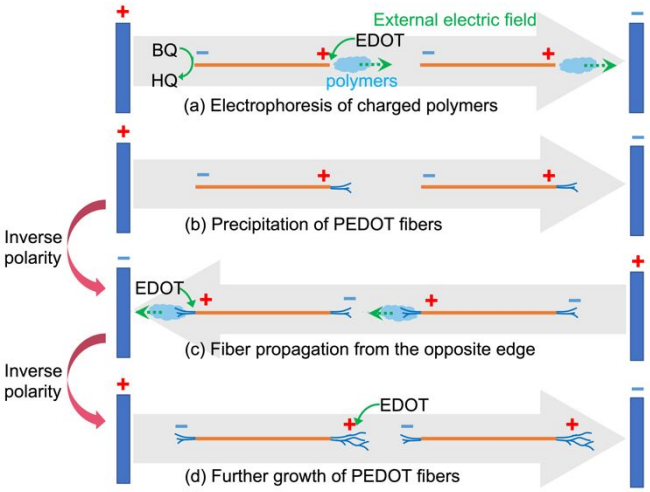

Fig. 6 Schematic of the AC-bipolar formation of PEDOT fibers assisted by the electrophoretic effect.[45] Reproduced with permission from ref. 45. Copyright 2016 Springer Nature.

Following this work, our group reported the fabrication of a linear PEDOT fiber using the AC-bipolar electropolymerization technique in a microspace (Fig. 7a).[47] The linear fibers were exclusively obtained by carrying out the polymerization in a microspace with a thickness of 30 μm, where monomer diffusion was extremely limited. In the microspace, the local concentration of monomer near the fibers decreased upon formation of the PEDOT fibers, inhibiting further branching; however, sufficient EDOT still surrounded the termini of the fibers. As a consequence, the PEDOT fibers propagated linearly without branching in the microspace.

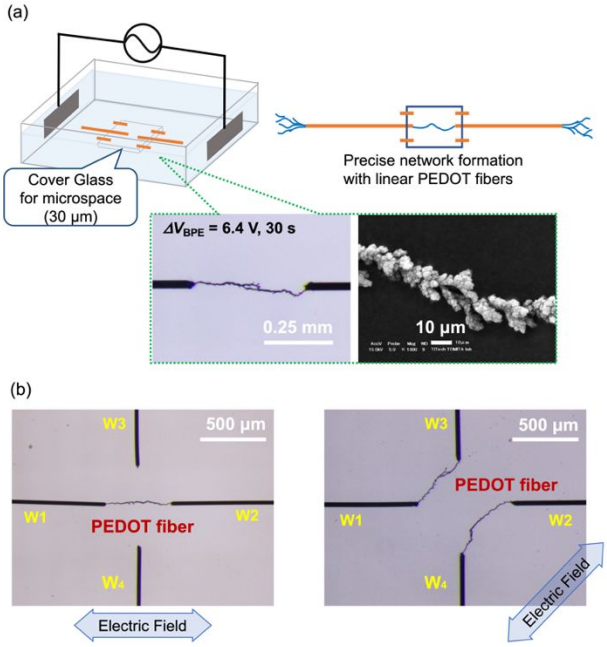

Fig. 7 Fabrication of linear PEDOT fibers with a microspace system:[47] (a) schematic of the setup and the optical and SEM images of obtained PEDOT fibers; (b) demonstration of the selective wiring of distinct Au wires in the presence of four independent wires. Reproduced with permission from ref. 47. Copyright 2017 Springer Nature.

Because of the linear nature of PEDOT formed under this condition, we successfully demonstrated the selective wiring of four independent Au wires by varying the direction of the external electric field. The selective formation of linear PEDOT instead of a dendritic structure provides a potential path to the establishment of wiring technology.

Under the AC-bipolar conditions, anodic and cathodic poles alternately appear at both edges of BPEs. Thus, designing a system using a cathodic reaction as well as anodic oxidation enables the fabrication of composite materials with sophisticated properties. On the basis of this concept, we carried out the electropolymerization of EDOT in the presence of $PtCl_6^{2-}$ ions, which were cathodically reduced to deposit metallic Pt nanoparticles (NPs) (Fig. 8a).[48] In addition, $PtCl_6^{2-}$ acted as a dopant and thus penetrated into the PEDOT fiber upon oxidation based on static interaction; the reductive deposition therefore proceeded efficiently. Using this method, PEDOT–Pt hybrid fibers were obtained, as confirmed by X-ray photoelectron spectroscopy (XPS), energy-dispersive X-ray spectroscopy (EDS), and SEM observations. XPS analysis suggested the dominant presence of Pt(0) species with a small amount of Pt^{4+} ion. EDS analysis indicated that S and Pt were widely dispersed over the material. SEM and transmission electron microscopy (TEM) observations revealed the presence of Pt-NPs with diameters of 5–10 nm (Fig. 8c). When $PtCl_6^-$ was substituted

with an Ag^+ salt, similar PEDOT fibers were obtained; however, aggregation of the Ag NPs (35–153 nm) was confirmed by SEM. In this case, the Ag^+ ions were not well dispersed in the PEDOT matrix via the anodic doping process. Because Pt- and Ag-NPs have various catalytic applications, the creation of Pt- and Ag-composite materials with PEDOT fibers represents a new approach to the development of novel devices and sensors.

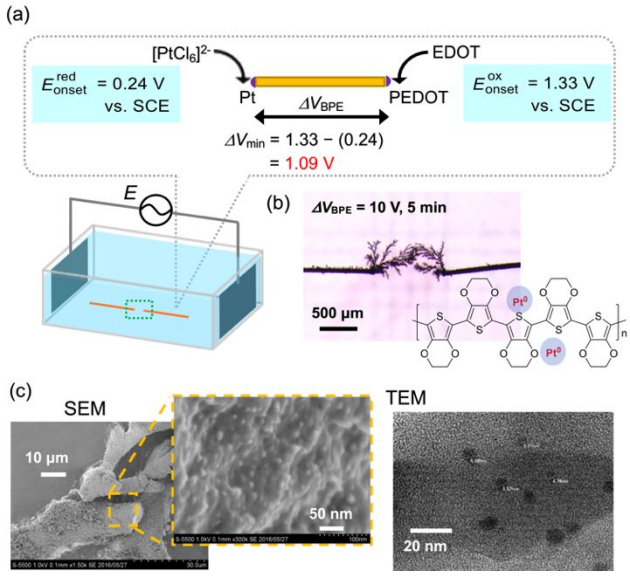

Fig. 8 Fabrication of PEDOT fiber–Pt NP composite material by AC-bipolar electrolysis:[48] (a) schematic of the reaction system; (b) optical image of the obtained PEDOT–Pt NP hybrid fibers; (c) SEM and TEM images of EDOT–Pt NP hybrid fibers. Reproduced with permission from ref. 48. Copyright 2018 American Chemical Society.

Another example of composite materials is PEDOT–poly(styrenesulfonate) (PEDOT:PSS), a well-known highly conductive material used in various devices.[48] AC-bipolar electropolymerization was performed in water containing PSS. The electrophoresis-assisted directed growth of PEDOT fibers was found to be applicable even in aqueous solutions. SEM analysis revealed a unique microstructure of PEDOT:PSS fibers with a smooth surface. Fourier transform infrared (FT-IR) spectra showed characteristic peaks of the incorporated PSS.

AC-bipolar electropolymerization with electrophoresis was also found to be effective for fabricating a PEDOT fiber array grown perpendicularly to the substrate (Fig. 9a).[19] In this system, a cylinder-type cell was used for the reaction, which enabled the local application of an electrical potential to the electrode surface via bipolar electrochemistry. This cell configuration was also proposed and developed by our group.[15,17,18] Using 1 mM Bu_4NClO_4/MeCN electrolyte solution containing 50 mM EDOT and 5 mM BQ, we carried out AC-bipolar electropolymerization with a cylindrical setup and an ITO plate positioned beneath the cylinder. Under an applied square-wave potential of 100 V with a frequency of 1 Hz, a PEDOT array was obtained within 45 min (Fig. 9b). The microstructure of the PEDOT fibers was similar to that of the fibers obtained in the linear bipolar cell systems.

The progress of the reaction can be divided into several steps. First, a PEDOT film is formed in a circular manner underneath the cylinder, reflecting the applied electrical potential. The film contains granular PEDOT based on the Stranski–Krastanov (S–K) mode of film formation. The granular morphology triggers perpendicular growth of the PEDOT fiber. The PEDOT fiber then grows in the perpendicular direction, guided by the external electric field and the electrophoretic effect. Notably, electrophoresis plays a critical role in this system because the fiber arrays need to grow against the gravitational force. Interestingly, a PEDOT film was not formed in the surrounding area of the ITO despite the surrounding area also functioning as an anodic surface under AC-bipolar conditions. Thus, this system enables site-selective modification of a conductive substrate with a PEDOT array.

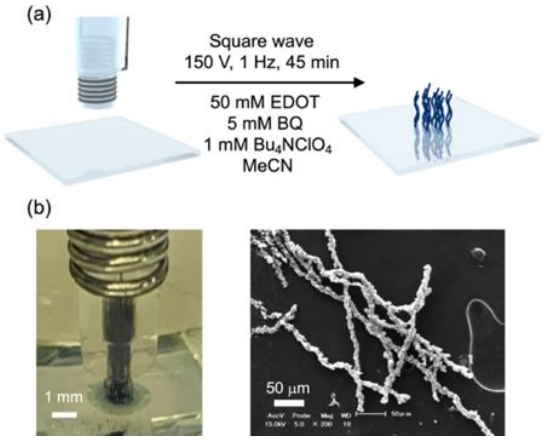

Fig. 9 Formation of a PEDOT fiber array by AC-bipolar electrolysis with a cylindrical setup:[19] (a) scheme of the reaction and (b) optical and SEM images of the PEDOT fiber array. Reproduced with permission from ref. 19. Copyright 2019 Royal Society of Chemistry.

6. Formation of PEDOT Films and Their Characteristics

The electrophoresis-assisted AC-bipolar electropolymerization has also been applied to the in-plane growth of PEDOT in the form of a thin film (Fig. 10a).[49] A PEDOT film in general is obtained through electropolymerization on a surface of a working electrode by a potential sweep method or electrolysis, where the film possesses no inherent anisotropy. However, a PEDOT film obtained by AC-bipolar electropolymerization possesses in-plane anisotropy, which can potentially lead to unique anisotropic electrical properties.

When a high concentration of EDOT monomer (150 mM) was used, we found that PEDOT preferentially forms a dendritic film rather than fibers under an applied square wave with a frequency of 1 or 5 Hz.[49] The film was grown on a glass substrate placed underneath the Au wire (Fig. 10a, top left). At higher frequencies (15 and 50 Hz), PEDOT was obtained as fibers; thus, both the monomer concentration and frequency are important parameters for the morphological selectivity. The obtained PEDOT film exhibited sufficient mechanical toughness to be used in further analyses and experiments. SEM and laser microscope measurements revealed that the thickness of the PEDOT film

was on the order of a few micrometers. The film formation was strongly dependent on the nature of the material of the underlying substrate. Insulating materials such as poly(vinyl chloride) (PVC), polypropylene (PP), polyethylene (PE), poly(tetrafluoroethylene) (PTFE), and poly(ethylene terephthalate) (PET) were tested in addition to glass (Fig. 10a). In-plane PEDOT films were successfully formed on the surfaces of PVC, PP, PE, and PET under the optimized conditions, whereas PEDOT fibers were obtained on PTFE, presumably because of the incompatibility between PTFE and PEDOT due to the oleophobic nature of PTFE. In fact, the use of a more hydrophobic monomer, *n*-decyl-modified EDOT, afforded the corresponding fibers on all of the investigated substrates under identical experimental conditions. Interestingly, the *n*-decyl-modified EDOT afforded a film structure on PTFE when a higher voltage was applied, indicating that the selectivity for forming fibers or a film is also determined by the balance between the reaction and deposition kinetics and the surface free energy, as well as by the monomer concentration.

A plausible mechanism for the formation of PEDOT films is described in Fig. 10b. The key factor determining the morphologies of polymers, *i.e.*, fiber or film, is the concentration of the EDOT monomer. At the lower EDOT monomer concentration (50 mM), PEDOT fibers are obtained because of repeated PEDOT generation and deposition at the growing tips of the fibers, as described in Fig. 6. However, at a higher concentration of EDOT monomer (150 mM), a greater amount of PEDOT is generated, followed by the deposition of PEDOT films onto the substrate in contact with the Au wire tip. In the next step, the propagating termini of the PEDOT films behave as BPEs, where further electropolymerization of EDOT proceeds and results in continuous film growth. Therefore, the PEDOT morphology is dependent on the applied frequency; *i.e.*, only lower frequencies afforded film growth due to the high concentration of PEDOT generated at each pulse.

ARTICLE

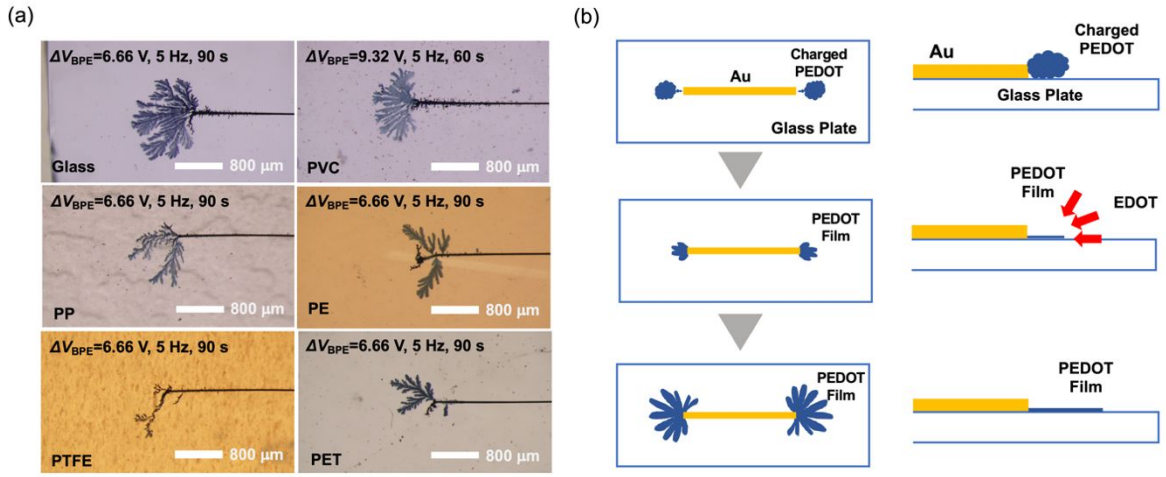

Fig. 10 PEDOT film formation under AC-bipolar electropolymerization:[49] (a) optical microscope images of the PEDOT film or PEDOT fibers formed on the various insulating substrates; (b) plausible mechanism for the formation of a PEDOT film. Reproduced with permission from ref. 49. Copyright 2018 American Chemical Society.

For the current technology to be applied to electrical wiring, understanding the electrical contact behavior between a PEDOT film and a metal is important. To this end, we investigated the electrical contact behaviors of PEDOT films in contact with Pt and Al.[50] A PEDOT film was prepared on a glass substrate (Fig. 11a), and Pt and Al plates were placed at the starting area and terminal area of the PEDOT film. The corresponding current–voltage (*I*–*V*) curves were then plotted. When two Pt plates were placed at both positions, ohmic contact behavior was observed. However, when two Al plates were placed in the same manner, Schottky contact behavior was observed. These results were attributed to the difference in the work functions of the Pt and Al plates. When Pt and Al were placed at the starting and terminal areas, Schottky contact behavior was observed (Fig. 11b). Interestingly, the opposite configuration of metal plates resulted in ohmic contact (Fig. 11b), suggesting anisotropic electrical properties of the PEDOT film.

The change in the *I*–*V* curve depending on the configuration of Pt and Al plates was attributed to the change of the Fermi level depending on the position of the PEDOT film. In a *p*-type semiconductor, the Fermi level is close to the level of the conduction band. On the basis of this idea, we were prompted to experimentally measure the local ionization energy using photoelectron yield spectroscopy in air (PYSA). PYSA measurements of the film revealed a gradient change of the local ionization potential of the PEDOT film, implying a gradient change of the Fermi level in a similar manner. Thus, we concluded that the PEDOT film obtained using this method showed a gradient change in its Fermi level over the propagation direction, which was originally generated by the gradient doping of the PEDOT during the polymerization process.

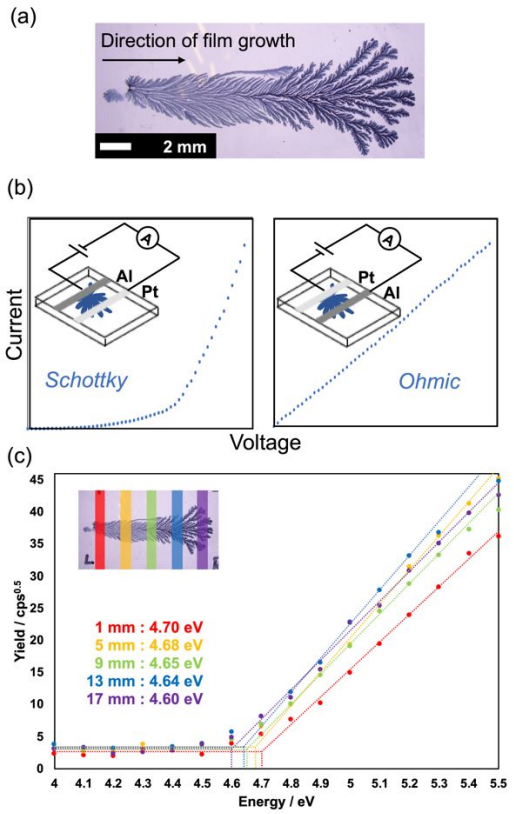

Fig. 11 Anisotropic electrical properties of the PEDOT film obtained by AC-bipolar electropolymerization.[50] (a) Photograph of the PEDOT film. (b) *I*–*V* curve of a PEDOT film. Al and Pt plates (left) or Pt and Al plates (right) were placed at the starting and terminal edges of the film,

respectively. (c) Local ionization potential of a PEDOT film fabricated by AC-bipolar electropolymerization, as determined using PYSA. Reproduced with permission from ref. 50. Copyright 2020 Elsevier.

7. Perspective

We have showcased recent advances in the fabrication of functional materials by bipolar electrolysis in synergy with electrophoresis. These examples indicate that, by careful design and execution, polymeric materials with unique structures are efficiently obtained in a straightforward manner. We also demonstrated the preliminary investigation on the anisotropic electrical character of the PEDOT films obtained by AC-bipolar electrolysis.[50] In contrast to the numerous researches on the properties of isotropic conductive polymers, characters of anisotropic conductive polymers are still not well studied. Our strategy enables easy access to the anisotropic PEDOT-based materials, thus opens a new door for the exploration of fundamental properties and application of anisotropic conductive polymeric materials.

Bipolar electrochemistry and electrophoresis are inherently highly compatible concepts. We hope that this paper gives some insight into the complex phenomena in bipolar systems and also gives new direction to the design of new systems for creating novel functional materials.

Acknowledgements

This work is supported by a Kakenhi Grant-in-Aid (JP17H03095 and JP20H02796) from the Japan Society for the Promotion of Science (JSPS), JST PRESTO (JPMJPR18T3), a Support for Tokyo Tech Advanced Researchers [STAR] grant funded by the Tokyo Institute of Technology Fund (Tokyo Tech Fund), and the JACI Prize for Encouraging Young Researchers (S.I.).

Notes and references

1 S. E. Fosdick, K. N. Knust, K. Scida and R. M. Crooks, *Angew. Chem. Int. Ed.*, 2013, **52**, 10438–10456.
2 G. Loget, D. Zigah, L. Bouffier, N. Sojic and A. Kuhn, *Acc. Chem. Res.*, 2013, **46**, 2513–2523.
3 N. Shida, Y. Zhou and S. Inagi, *Acc. Chem. Res.*, 2019, **52**, 2598–2608.
4 S. R. Waldvogel, S. Lips, M. Selt, B. Riehl and C. J. Kampf, *Chem. Rev.*, 2018, **118**, 6706–6765.
5 L. Koefoed, S. U. Pedersen and K. Daasbjerg, *Curr. Opin. Electrochem.*, 2017, **2**, 13–17.
6 K. Hiramoto, E. Villani, T. Iwama, K. Komatsu, S. Inagi, K. Y. Inoue, Y. Nashimoto, K. Ino and H. Shiku, *Micromachines*, 2020, **11**, 530.
7 L. Bouffier, S. Arbault, A. Kuhn and N. Sojic, *Anal. Bioanal. Chem.*, 2016, **408**, 7003–7011.
8 F. Mavré, R. K. Anand, D. R. Laws, K. F. Chow, B. Y. Chang, J. A. Crooks and R. M. Crooks, *Anal. Chem.*, 2010, **82**, 8766–8774.
9 S. Inagi, *Polym. J.*, 2016, **48**, 39–44.
10 L. Bouffier, N. Sojic and A. Kuhn, *Electrophoresis*, 2017, **38**, 2687–2694.
11 N. Shida, F. Kitamura, T. Fuchigami, I. Tomita and S. Inagi, *ChemElectroChem*, 2016, **3**, 465–471.
12 S. Inagi, Y. Ishiguro, M. Atobe and T. Fuchigami, *Angew. Chem. Int. Ed.*, 2010, **49**, 10136–10139.
13 Y. Ishiguro, S. Inagi and T. Fuchigami, *Langmuir*, 2011, **27**, 7158–7162.
14 N. Shida, Y. Ishiguro, M. Atobe, T. Fuchigami and S. Inagi, *ACS Macro Lett.*, 2012, **1**, 656–659.
15 S. Inagi, Y. Ishiguro, N. Shida and T. Fuchigami, *J. Electrochem. Soc.*, 2012, **159**, G146–G150.
16 K. Miyamoto, H. Nishiyama, I. Tomita and S. Inagi, *ChemElectroChem*, 2019, **6**, 97–100.
17 Y. Ishiguro, S. Inagi and T. Fuchigami, *J. Am. Chem. Soc.*, 2012, **134**, 4034–4036.
18 N. Shida, Y. Koizumi, H. Nishiyama, I. Tomita and S. Inagi, *Angew. Chem. Int. Ed.*, 2015, **54**, 3922–3926.
19 Y. Zhou, N. Shida, Y. Koizumi, T. Watanabe, H. Nishiyama, I. Tomita and S. Inagi, *J. Mater. Chem. C*, 2019, **7**, 14745–14751.
20 W. Gao, K. Muzyka, X. Ma, B. Lou, G. Xu, *Chem. Sci.* 2018, **9**, 3911–3916.
21 W. Qi, J. Lai, W. Gao, S. Li, S. Hanif, G. Xu, *Anal. Chem.* 2014, **86**, 8927–8931.
22 L. Qi, Y. Xia, W. Qi, W. Gao, F. Wu, G. Xu, *Anal. Chem.* 2015, **88**, 1123–1127.
23 G. Loget and A. Kuhn, *Nat. Commun.*, 2011, **2**, 535.
24 G. Loget and A. Kuhn, *Lab Chip*, 2012, **12**, 1967–1971.
25 K. F. Chow, F. Mavré, J. A. Crooks, B. Y. Chang and R. M. Crooks, *J. Am. Chem. Soc.*, 2009, **131**, 8364–8365.
26 K. Ino, R. Yaegaki, K. Hiramoto, Y. Nashimoto and H. Shiku, *ACS Sensors*, 2020, **5**, 740–745.
27 F. Mavré, K. F. Chow, E. Sheridan, B. Y. Chang, J. A. Crooks and R. M. Crooks, *Anal. Chem.*, 2009, **81**, 6218–6225.
28 J. C. Bradley, H. M. Chen, J. Crawrford, J. Eckert, K. Ernazarova, T. Kurzeja, M. Lin, M. McGee, W. Nadler and S. G. Stephens, *Nature*, 1997, **389**, 268–271.
29 J.-C. Bradley, *J. Electrochem. Soc.*, 1998, **145**, L45.
30 J. C. Bradley, Z. Ma and S. G. Stephens, *Adv. Mater.*, 1999, **11**, 374–378.
31 J. C. Bradley, S. Dengra, G. A. Gonzalez, G. Marshall and F. V. Molina, *J. Electroanal. Chem.*, 1999, **478**, 128–139.
32 J.-C. Bradley, *J. Electrochem. Soc.*, 1999, **146**, 194.
33 G. Loget, J. Roche, E. Gianessi, L. Bouffier and A. Kuhn, *J. Am. Chem. Soc.*, 2012, **134**, 20033–20036.
34 C. Kumsapaya, M. F. Bakaï, G. Loget, B. Goudeau, C. Warakulwit, J. Limtrakul, A. Kuhn and D. Zigah, *Chem. Eur. J.*, 2013, **19**, 1577–1580.
35 G. Loget, J. Roche and A. Kuhn, *Adv. Mater.*, 2012, **24**, 5111–5116.
36 C. Ulrich, O. Andersson, L. Nyholm and F. Björefors, *Angew. Chem. Int. Ed.*, 2008, **47**, 3034–3036.
37 A. Lundgren, S. Munktell, M. Lacey, M. Berglin and F. Björefors, *ChemElectroChem*, 2016, **3**, 378–382.

38 M. Ongaro, J. Roche, A. Kuhn and P. Ugo, *ChemElectroChem*, 2014, **1**, 2048–2051.
39 J. Roche, G. Loget, D. Zigah, Z. Fattah, B. Goudeau, S. Arbault, L. Bouffier and A. Kuhn, *Chem. Sci.*, 2014, **5**, 1961–1966.
40 M. Atobe, S. Iizuka, T. Fuchigami and H. Yamamoto, *Chem. Lett.*, 2007, **36**, 1448–1449.
41 M. Atobe, N. Yoshida, K. Sakamoto, K. Sugino and T. Fuchigami, *Electrochim. Acta*, 2013, **87**, 409–415.
42 Y. Koizumi, H. Nishiyama, I. Tomita and S. Inagi, *Chem. Commun.*, 2018, **54**, 10475–10478.
43 Y. Zhou, N. Shida, Y. Koizumi, K. Endo, I. Tomita and S. Inagi, *Macromolecules*, 2020, **53**, 8123–8130.
44 Y. Koizumi, N. Shida, I. Tomita and S. Inagi, *Chem. Lett.*, 2014, **43**, 1245–1247.
45 Y. Koizumi, N. Shida, M. Ohira, H. Nishiyama, I. Tomita and S. Inagi, *Nat. Commun.*, 2016, **7**, 10404.
46 S. Inagi, *Polym. J.*, 2019, **51**, 975–981.
47 M. Ohira, Y. Koizumi, H. Nishiyama, I. Tomita and S. Inagi, *Polym. J.*, 2017, **49**, 163–167.
48 Y. Koizumi, M. Ohira, T. Watanabe, H. Nishiyama, I. Tomita and S. Inagi, *Langmuir*, 2018, **34**, 7598–7603.
49 T. Watanabe, M. Ohira, Y. Koizumi, H. Nishiyama, I. Tomita and S. Inagi, *ACS Macro Lett.*, 2018, **7**, 551–555.
50 N. Shida, T. Watanabe, I. Tomita and S. Inagi, *Synth. Met.*, 2020, **266**, 116439.

Authors' bio

Naoki Shida received his PhD from the Tokyo Institute of Technology in 2016 under the supervision of Prof. Shinsuke Inagi. His thesis focused on the gradient modification of a substrate surface by means of bipolar electrochemistry. He then worked as a postdoctoral scholar (Research Fellowship for Young Scientists, JSPS) at both the Tokyo University of Agriculture and Technology and the California Institute of Technology. Afterward, he joined the group of Prof. Shinsuke Inagi as a Specially Appointed Assistant Professor in 2018. His research interests are based on electrosynthesis and cover the areas of organic chemistry, polymer science, and inorganic chemistry.

Shinsuke Inagi received his PhD from Kyoto University in 2007. After a JSPS postdoctoral research fellowship at Kyoto University, he joined the group of Prof. Toshio Fuchigami as an Assistant Professor at the Tokyo Institute of Technology in 2007. He was promoted to Lecturer in 2011, then to Associate Professor in 2015. He is concurrently a PRESTO researcher at the Japan Science and Technology Agency (JST) and has held this position since 2018. His current research interests include electrosynthesis of functional materials by means of bipolar electrochemistry. He was the recipient of the Tajima Prize of the International Society of Electrochemistry (ISE) in 2019.

TOC

The synergistic effect of bipolar electrochemistry and electrophoresis enables facile access to various anisotropic functional materials.